Hydro-geomorphic controls of greenhouse gas fluxes in riparian buffers of the White River watershed, IN (USA)

AUTHORS: P.-A. Jacinthe [a*], P. Vidon [b]

ADDRESSES OF AUTHORS:

[a] Center for Earth and Environmental Sciences, Indiana University Purdue University, Indianapolis, IN 46202

[b] Department of Forest and Natural Resources Management, SUNY-ESF, Syracuse, NY

CORRESPONDING AUTHOR:

*Dr. Pierre-André Jacinthe, Department of Earth Sciences, Indiana University Purdue University Indianapolis (IUPUI), 723 W. Michigan Street, SL 118, Indianapolis, IN 46202

Phone: (317) 274-7969; Fax: (317) 274 7966; E-mail: pjacinth@iupui.edu

Number of pages: 27 (including abstract and references)

Number of figures: 6

Number of Tables: 8

This is the author's manuscript of the article published in final edited form as:

Jacinthe, P.-A., & Vidon, P. (2017). Hydro-geomorphic controls of greenhouse gas fluxes in riparian buffers of the White River watershed, IN (USA). Geoderma, 301(Supplement C), 30–41. https://doi.org/10.1016/j.geoderma.2017.04.007

ABSTRACT

Riparian ecosystems are defined by the nature and regularity of the interactions between a given river system and its floodplains, and past studies have often presented vegetation cover as the exclusive expression of these interactions. There has been to our knowledge, no systematic attempt at linking greenhouse gases (GHG) fluxes and types of riparian buffers. The present study was conducted to investigate the intensity and seasonality of carbon dioxide (CO_2), methane (CH_4) and nitrous oxide (N_2O) fluxes in riparian buffers in three common hydro-geomorphic settings (HGM) across the White River watershed (Indiana, USA). These classes included riparian sites located: (i) in till plain depressions near 1st order streams (HGM-1), (ii) in incised narrow valleys with thin alluvium layers above glacial till (HGM-2), and (iii) along 3rd-4th order streams in broad floodplains with thick alluvial and glacial outwash deposits (HGM-3). For each class, 3 sites were selected and GHG fluxes were measured during the wet (May) and dry seasons (August). Strong relationships were found between GHG fluxes, soil properties and environmental factors, but these relationships varied with season and gas species, making it challenging to rely on these relationships for GHG fluxes upscaling. Analysis of variance and discriminant analysis showed that the HGM-defined riparian buffers were distinct in terms of GHG flux intensity. Regardless of season, the HGM-1 sites emitted CO_2 at rates 1.6 times higher than at the other sites, likely due to difference in soil C quality. During the wet season, N_2O emission was significantly higher at the HGM-3 than at the other sites (0.88 vs 0.27 mg N m^{-2} d^{-1}), and was negatively related with the gradient of the adjacent channel (r^2: 0.69). The riparian buffers acted as CH_4 sinks, with the HGM-2 sites exhibiting CH_4 uptake rates significantly greater than the other riparian types (-0.80 vs -0.34 mg CH_4-C m^{-2} d^{-1}). The consistency of these

results underscore the potential of an HGM-based monitoring approach to derive watershed-scale GHG budgets for riparian buffers.

Keywords: greenhouse gases; riparian buffer classes; hydro-geomorphology; channel gradient

1. Introduction

Because of their location at the interface between terrestrial and aquatic ecosystems, riparian zones act as natural filters and contribute to the retention of pollutants which otherwise would have been transferred to adjacent surface water bodies. While the water quality protection benefits of riparian buffers are well documented (Gold et al., 2001; Vidon and Hill, 2004; Dosskey et al., 2010), significant gaps exist in our understanding of the intensity and regulation of greenhouse gases (GHG) production in these ecosystems. Anaerobic conditions in riparian soils are favorable for the removal of NO_3^- via denitrification, but could also enhance the production of nitrous oxide (N_2O) and methane (CH_4) (Gold et al., 2001; Jacinthe et al., 2015). Accelerated transfer of these gases into the atmosphere is a concern given the steady increase in their atmospheric concentration, their global warming potential (warming potential of N_2O and CH_4 is respectively 298 and 28 times that of CO_2), and their implication in stratospheric ozone depletion (IPCC, 2013).

Riparian ecosystems are often categorized on the basis of the type, density, and diversity of the vegetation cover they support (e.g., grass, forest), but relationships between vegetation attributes and GHG fluxes in riparian buffers have been inconsistent. Hopfensperger et al. (2009) found a negative trend between percent vegetation cover and N_2O fluxes in forested riparian wetlands. Hefting et al. (2003*)* reported significantly higher N_2O emission in forested than in grass-covered riparian buffers, suggesting an effect of vegetation type. Similarly, higher rates of N_2O

emission were measured in riparian ecosystems supporting mesquite (*Prosopis velutina*) vegetation compared to other plant communities (McLain and Martens, 2006). van Haren et al. (2010) concluded that tree species was the most important predictor of N_2O fluxes in central Amazonian riparian forests. In contrast, Walker et al. (2002) reported limited effect of land cover and land-use on N_2O emission in grazed and restored riparian grassland. Likewise, Addy et al. (1999) found limited difference between forested and grassed riparian buffers with regard to NO_3^- removal and N_2O emission. However, past studies in the eastern USA (Jacinthe et al., 1998) and southern Canada (Vidon and Hill, 2004) have shown that hydrology and geologic settings (till, outwash, alluvial) are strong predictors of the N removal capacity of riparian buffers. These results concur with the conclusion of Clement et al. (2002) that topography, rather than vegetation, is the most important controlling factor of denitrification in riparian buffers.

Several studies have reported strong relationships between vegetation type and CH_4 fluxes in peatlands leading to the suggestion that vegetation cover can serve as a valid proxy for large-scale assessment of CH_4 budget in these ecosystems (Dias et al., 2010; Couwenberg et al., 2011). However, in riparian buffers, similar linkages are less frequently identified. Across several riparian buffers in Iowa, no significant difference was detected among different types of vegetation cover with respect to CH_4 flux (Kim et al., 2010). Work in riparian sites of south-central Indiana (Jacinthe et al., 2012; Fisher et al., 2014; Jacinthe et al., 2015) has also shown limited effect of vegetation type (grass vs forest) on either CO_2 and CH_4 fluxes, but these studies have shown that flood frequency was the determining factor of GHG dynamics in these ecotones. Flood events result in the redistribution of materials across affected riparian landscapes, influence the spatial distribution of soil properties, and have both short-term and long-lasting effects on soil microbial processes controlling GHG production (Samaritani et al., 2011; Audet et

al., 2013). For example, similar to the observations made in riparian buffers in Indiana, higher rates of CO_2 emission were recorded in flood-affected riparian buffers compared to flood-protected riparian sites adjacent to channelized sections of the Thur River in Switzerland (Samaritani et al., 2011). Further, under similar soil moisture and temperature, significantly lower rates of soil CH_4 uptake were measured in flood-affected than in flood-protected riparian sites, suggesting a long-lasting effect of flood events on the soil methanotrophic community (Jacinthe, 2015).

Because landscape hydrogeomorphic characteristics (channel slope, stream bank geometry, topography, surficial geology, soil types) influence stream-riparian interactions (including flooding frequency), we argue that a hydrogeomorphic (HGM) framework to classify riparian zones at the watershed scale (Gold et al., 2001; Vidon and Hill, 2004) could provide a useful approach (more than land-cover) to monitor GHG dynamics in riparian buffers and elucidate the underlying factors controlling the variability of GHG fluxes in these ecosystems. This classification could also provide the basis for regional-scale inventories of GHG emission from riparian buffers. Through integration of river valley geometry, channel gradient and discharge data (to derive flood duration and height), such a classification was developed for the White River watershed in Indiana (Panunto, 2012). The classification, mostly used previously for insurance and flood management purposes (Woltemade and Potter, 1994), is based on a river valley sequencing approach that accounts for longitudinal variations in the morphology (gradient, storage capacity) of consecutive valley segments along a river to predict flood magnitude and duration (Bedient et al, 2007). For example, flood risk is high along a low-gradient valley segment that is located downstream from a high-gradient segment. However, flood risk is much lower when a high-gradient segment is downstream from either a low-gradient or another high-gradient

segment. Using the various combinations of channel gradient (low, high) and valley geometry (narrow, wide) to derive floodplain hydroperiods in different sections of the White River watershed, five major types of riparian buffers were identified (Panunto, 2012). In the present study, we aim to determine whether these types of riparian buffers differ in terms of their GHG emission potential. To that end, we monitored GHG fluxes and measured relevant soil properties at different sites representative of the three most common riparian buffers identified in the watershed.

2. Material and Methods

2.1. Description of the study sites

The study was conducted at nine riparian sites (Fig. 1, Table 1), located within a 70-km radius, across the White River watershed in Indiana, USA (humid temperate climate, mean annual temperature of 11^{o}C, annual rainfall of 1044 mm). The sites were selected to represent the three most common hydrogeomorphic (HGM) settings in which riparian buffers occur in the watershed (Panunto, 2012), and more generally in Illinois, Indiana, and Ohio given regional similarities in climate, land-use and glaciation history (Antevs, 1929). These include: (i) riparian buffers in till plains depression along first-order streams and agricultural drainage ditches (HGM-1); (ii) riparian buffers in incised narrow valleys bordered by steep bluffs, most commonly occurring along second-order streams in the transition zone from till plains to outwash plains (HGM-2); and (iii) riparian buffers in broad floodplains filled with outwash deposits along 3rd/4th order segments of the White River (HGM-3). Stream channels along the HGM-1 buffers are often dredged and deepened to protect nearby crop fields from flooding, while subsurface drains are most often present in the adjacent fields (Franzmeier and Kladivko, 2001). Due to their topography and longitudinal profile of the adjacent river channels, flood

events at HGM-2 are generally of short duration (< 1 day). However, due to their location along larger river segments and the geometry of adjacent channel, the HGM-3 buffers are flood-prone and can remain flooded for several consecutive days during an event (Liu et al., 2014; Jacinthe, 2015). Information related to flood regime at the riparian buffers was obtained from Panunto (2012), and previous studies conducted at nearby sites (Jacinthe et al., 2012; Fisher et al., 2014; Liu et al., 2014; Vidon et al., 2014; Jacinthe, 2015; Jacinthe et al., 2015). River geometry information was derived from StreamStats (http://water.usgs.gov/osw/streamstats/indiana.html) and summarized in Table 1.

For each HGM type (Table 1), three riparian buffers were selected on the basis of landscape features, and local flood dynamics (Panunto, 2012). The HGM-1 riparian sites selected for this investigation consisted of grass-dominated riparian strips (8-20 m wide) adjacent to actively-managed croplands (typically with subsurface drainage) under corn (*Zea mays*)-soybean (*Glycine max*) rotation as is most common for HGM-1 riparian zones in the region. Vegetation in these riparian buffers predominantly consisted of orchard grass (*Dactylis glomerata* L.), blue grass (*Poa annua* L.) and a few interspaced shrubs. The HGM-2 and HGM-3 sites were variably flooded secondary-growth deciduous forests, mostly located within municipal parks and other protected areas as is common for most HGM-2 and HGM-3 riparian buffers in the region. Although small differences in topography may occur within sites, HGM-2 sites generally present a concave topography (steep embankment and flat riparian zone), while HGM-3 sites generally present a mostly flat topography. The tree stands at the HGM-3 sites were generally denser and more mature (> 80 y old) than at the HGM-2 sites with the most common tree species being silver maple (*Acer saccharinum*), American beech (*Fagus sylvatica* L.), American sycamore (*Platanus occidentalis*), white oak (*Quercus alba*), bur oak (*Quercus macrocarpa*) and red ash

(*Fraxinus pennsylvanica*). At the HGM-1 sites, soils are classified as Brookston (Typic Argiaquolls), deep and poorly-drained soils developed from loamy glacial till and loess in depressional areas. Due to natural soil drainage restriction, adjacent agricultural fields are equipped with subsurface tile drains, and the subsurface drainage network often runs underneath the riparian buffer. At the HGM-2 and HGM-3 sites, the dominant soil types are Genesee silt loam (Fluventic Eutrudepts) and Stonelick sandy loam (mesic Typic Udifluvents), moderately well drained soils developed on alluvium (HGM-2) or glacial outwash (HGM-3).

2.2. Monitoring of gas fluxes

Gas fluxes were measured using the static chamber method in May 2011 and in August 2011, representing respectively the wet and the dry periods that typically characterize the growing season in the region. At each site, eight chambers were installed and were distributed so as to capture topographical variability within each site. Chambers were installed 3-5 days prior to making measurements of GHG fluxes. Chambers (diameter: 30 cm; height above ground: 18 cm; depth of insertion into the ground: 5 cm) were made of a polyvinyl chloride (PVC) pipe and a PVC lid to close the chamber. The lid was fitted with a gasket at its underside edge to make an air-tight seal with the chamber and with a butyl rubber septa at its center to form a sampling port. Air samples (~ 10 mL) were taken from each chamber headspace at 0, 20, 40 and 60 min after closure, and stored in pre-evacuated 7-mL vials fitted with butyl rubber septa. For most sampling dates, air samples were analyzed overnight, upon return from the field. Details regarding the construction, ground insertion and operation of the gas chambers are available elsewhere (Fisher et al., 2014). From variation in gas concentration inside the chamber, gas flux (F, mass of gas m^{-2} d^{-1}) was computed using the equation:

$$F = (\frac{\Delta C}{\Delta t})(\frac{V}{A})k$$

where $\Delta C/\Delta t$: rate of change in GHG concentration inside the chamber (mass GHG m^{-3} air min^{-1}) obtained by linear regression, V: chamber volume ($12x10^{-3}$ m^3), A: area circumscribed by the chamber ($7.1x10^{-2}$ m^2), and k: time conversion factor (1440 min d^{-1}). A positive value of F corresponds to a net emission of gas from soil into the atmosphere. Conversely, a negative F value corresponds to a net transfer (uptake) of gas from the atmosphere into the soil.

Air samples were analyzed for CO_2, CH_4 and N_2O using a Varian CP-3800 gas chromatograph (GC) interfaced with a CombiPal autosampler (CTC Analytics, Zurich, Switzerland) and operating at an oven temperature of 90 ^oC. The GC was fitted with a thermal conductivity detector (100 ^oC, for CO_2 detection), a flame ionization detector (100 ^oC, for CH_4 detection) and an electron capture detector (300 ^oC, for N_2O detection). The stationary phase consisted of a pre-column (L: 0.3 m; id: 2 mm) and an analytical column (L: 1.8 m; id: 2 mm) packed with Porapak Q (80-100 mesh). Carrier gases included UHP N_2 (60 mL min^{-1}) and UHP He (60 mL min^{-1}), and the flame gases for the FID detector were hydrogen and hydrocarbon-free compressed air. The GC was calibrated using standard gases obtained from Alltech (Deerfield, IL). The GC system (detection limit: 20 µL CO_2 L^{-1}, 0.12 µL CH_4 L^{-1}, 0.03 µL N_2O L^{-1}) was calibrated with standards obtained from Alltech (Deerfield, IL).

2.3. Soil properties

At each sampling occasion, surface soil temperature (0-20 cm) was measured next to each chamber with a portable soil thermometer (Cole Parmer, Vernon Hills, IL), and soil samples (0-20 cm) were collected for determination of gravimetric soil moisture content and mineral nitrogen. The samples collected during the August sampling event (dry season) were

also used for determination of soil pH, texture, C and N content, dissolved organic carbon and denitrification enzyme activity. Soil pH was determined with a pH electrode using a 2:1 water to soil suspension. Soil texture was determined by sieving for the sand fraction (>53 µm) and by the hydrometer method for the silt and clay fractions following organic matter removal with hydrogen peroxide and dispersion of soil samples with sodium hexametaphosphate. Total carbon and total nitrogen (TN) was determined by dry combustion (960 ^{o}C) of finely-ground (150 µm) soil samples on a Vario TOC C-N analyzer in solid mode (Elementar Americas, NJ). Fresh soil (~20 g moist) was extracted with 2 M KCl, and the extract analyzed for NO_3^- and NH_4^+ using a photometric analyzer (Aquakem 20, EST Analytical, Fairfield, OH). Field moist samples were also extracted with deionized water (10 g of soil, 20 mL of water), and the filtrate (0.45 µm GF filter) analyzed for dissolved organic C (DOC) using a Vario TOC C-N analyzer in liquid mode (Elementar Americas, NJ). Gravimetric moisture content at the time of GHG measurements was determined by oven drying of moist soil samples at 105 ^{o}C for 48 h in an oven. All results are reported on the basis of dry soil.

Denitrification activity was also measured in the soil samples collected during the dry season sampling (August 2011). Denitrification was measured using the acetylene (C_2H_2) inhibition technique (Smith and Tiedje, 1979). Duplicate field-moist soil samples (10 g) were transferred into serum bottles (160 mL) and slurried with 10 mL of denitrification media (per liter: 1.5 g KNO_3, 1 g glucose, 0.25 g chloramphenicol). Bottles were capped with butyl rubber septa and crimp-sealed. Each bottle headspace was evacuated and flushed with N_2 gas (3 times for a total of 15 min) to create anaerobic conditions. Each bottle was amended with C_2H_2 (10 kPa) and incubated at room temperature (22 ^{o}C). Bottle headspace was periodically sampled over

a 7-day period to determine N_2O and CO_2 production rates. Gas samples were stored in evacuated glass vials and analyzed for N_2O and CO_2 by gas chromatography.

2.4. Data analysis

The data were analyzed using descriptive statistics, analysis of variance (ANOVA), regression models, and discriminant analysis (DCA). ANOVA was performed to assess the effect of riparian zone type (HGM) and season on GHG fluxes and related soil properties. In this analysis, HGM and season were used as the main factors. ANOVA and regression analysis were conducted with the SAS software for Windows (Version 9.3, SAS Institute Inc., Cary, N.C., USA) using the GLM (general linear modeling) and REG procedures, respectively. Statistical significance was determined at the 95% confidence level. In order to validate our general hypothesis that HGM types are distinct in terms of GHG dynamics, we conducted discriminant analysis (DCA) using the CO_2, CH_4 and N_2O data to determine to what extent the riparian sites are separated based on their HGM settings. Before conducting DCA, data were normalized by subtracting the mean value to each individual value and dividing by the standard deviation (Zimmer and Lautz, 2013). Discriminant analysis was performed with PAST3 statistical software (Hammer et al., 2001).

3. Results

3.1. General soil properties

Soil pH ranged from 5.7 to 7.5 (Table 2), and was on average slightly lower (6.7±0.7) at the HGM-1 than at the other riparian sites (7.2±0.1). In general, soils have a higher sand content at the HGM-2 buffers and are more fine-textured (clay+silt: 62% on average) at the HGM-1 sites

(Table 2). The riparian sites significantly differed ($P<0.001$) with respect to organic C (SOC) concentration and C/N ratio of the soil organic matter. On average, SOC content was 1.3 times higher at HGM-3 than at the other types of riparian sites (Table 2). The lowest concentrations of SOC (range: 32.1-35.8 g C kg^{-1}) and DOC (11.7 - 33.7 mg C kg^{-1}) were recorded at the sandy-loam HGM-2 sites (Tables 2 and 3).

The riparian sites also significantly differed with regard to soil respiration ($P<0.001$), and denitrification enzyme activity ($P<0.004$). Overall, for the soil parameters linked to organic C availability and microbial activity, measured level was consistently highest at the HGM-1 and lowest at the HGM-2 sites (Table 2). Soil respiration and DEA were strongly related (r^2: 0.52; $P < 0.001$), but relationships of these soil biochemical properties with DOC and SOC were not significant. DEA was positively correlated with soil clay content (r^2: 0.48).

Significant difference ($P<0.002$) among the riparian buffers was observed with respect to both NH_4^+ and NO_3^- concentration (Table 3). Irrespective of the season, NH_4^+ and NO_3^- were equally represented in the mineral N pool at the HGM-2 sites, whereas NH_4^+ was dominant at the HGM-1 sites and NO_3^- at the HGM-3 sites (Table 3). The NH_4^+/ NO_3^- ratio of mineral N was correlated negatively with the C/N ratio of soil organic matter, and positively with soil respiration (Tables 2 and 3).

3.2. Environmental conditions: soil moisture and temperature

The sampling periods, a priori designated as wet season and dry season, presented drastically different weather conditions. The spring/early summer of 2011 was wet with total rainfall (Indianapolis airport, 12-40 km from the study sites) of 329 mm in April-May. In contrast the July-August period of 2011 was very dry with a total rainfall of 40 mm. Normal

precipitation during these periods is 225 mm and 195 mm, respectively. Air temperature was near normal in April-May averaging 15.5 ^{o}C, whereas the July-August period was marked by warmer than normal temperature (average: 27.8 ^{o}C; normal: 24.1 ^{o}C).

Soil temperature at the riparian sites was 5.6 ^{o}C warmer during the dry than in the wet season (Table 4). In both seasons, soil moisture was generally highest at the clay-loam HGM-1 sites and lowest at the sandy-loam HGM-2 sites. Soil was anomalously dry during the dry season especially at sites with coarse soil texture (mean: 0.19 g H_2O g^{-1} soil; 33% less moisture than in the wet season; Table 4). The largest seasonal variation in soil moisture was observed at the HGM-3 sites. In the month prior to the wet season monitoring of GHG flux, the HGM-3 sites were likely flooded on two occasions (April 20-23 and April 27-30) as indicated by stream discharge in excess of bankfull (~400 m^3 s^{-1}; USGS gauging station 3353000, http://waterwatch.usgs.gov).

3.3. Greenhouse gases fluxes

Measured gas fluxes exhibited considerable between-site and within-site variability (Figs. 2 - 4). The intensity of CO_2 emission did not significantly vary between the wet and dry season (3.77 vs 3.44 g CO_2-C m^{-2} d^{-1}), but CO_2 emission was significantly higher at the HGM-1 buffers than at the other sites (Table 5 and Fig. 2). CO_2 flux was positively related to soil moisture during the dry season (r^2: 0.48), but not during the wet season (Table 6). No relationship between CO_2 flux and soil temperature was detected in either season. However, in both seasons, significant positive relationships (r^2: 0.48-0.49, $P<0.05$) were found between CO_2 flux and soil NH_4^+concentration.

Although emission of CH_4 was detected in a few instances (2.2% of cases), soils at the riparian buffers were net CH_4 sinks (Fig. 3). Methane fluxes ranged from -2.21 mg CH_4-C m^{-2} d^{-1} (site 4, dry season) to +0.38 mg CH_4-C m^{-2} d^{-1} (site 8, wet season). ANOVA showed a significant effect of both riparian buffer type and season on CH_4 fluxes. Across study sites, the rate of CH_4 uptake was 2-times higher in the dry than in the wet season (Table 5). Although not significant, negative relationships were observed between soil sand content and CH_4 fluxes (r^2: 0.32, $P<0.10$ during the wet season; r^2: 0.21, $P<0.20$ during the dry season). Consequently (Fig. 3), in both the wet (-0.53 mg CH_4-C m^{-2} d^{-1}) and dry season (-1.11 mg CH_4-C m^{-2} d^{-1}), CH_4 consumption was significantly greater at the sandy-loam HGM-2 than at the other types of riparian buffers (-0.21 and -0.47 mg CH_4-C m^{-2} d^{-1} during the wet and dry periods, respectively).

At the riparian sites, N_2O fluxes ranged between -0.50 and 4.51 mg N_2O-N m^{-2} d^{-1} (Fig. 4). Overall, the within-site spatial variability of N_2O fluxes was greatest during the wet season and at the HGM-3 sites (Fig. 4). Several instances (10.4% of the cases) of negative N_2O fluxes were recorded, the quasi-totality of them at site 4 and site 6. ANOVA showed a significant effect of both riparian buffer type and season on N_2O fluxes (Table 5). Across study sites, the riparian buffers emitted N_2O at a rate that was almost 2-times higher in the wet than in dry season (0.48 vs 0.26 mg N_2O-N m^{-2} d^{-1}, respectively; Table 5). During both seasons, the lowest average N_2O flux was measured at the HGM-2 sites (Fig. 4 and Table 5). During the wet season, N_2O emission was significantly greater at the HGM-3 than at the HGM-1 sites (0.88 vs 0.31mg N_2O-N m^{-2} d^{-1}, respectively; Fig. 4), but during the dry season there was no difference in N_2O emission between these two types of buffers (0.30 vs 0.36 mg N_2O-N m^{-2} d^{-1}, respectively; Fig. 4). During the wet season, N_2O flux correlated positively with soil NO_3^- concentration (r^2: 0.83, $P< 0.001$) and negatively with the slope gradient of adjacent channel (r^2:0.69, $P< 0.001$; Table 6

and Fig. 5). During the dry season, however, N_2O flux correlated with soil clay content, NH_4^+concentration, and soil respiration (Table 6).

Despite some degree of overlap, the DCA yielded discernible separations among the three types of riparian buffers on the basis of GHG fluxes (Fig. 6). Overall, 73% of measurements from HGM-1 sites were correctly classified, but only 60% of measurements from HGM-2 and HGM-3 were correctly classified, suggesting some degree of similarity between these two types of riparian buffers.

3.4. Previously published data

To evaluate the variability of the observed trend between gas flux and HGM class, data from the present investigation was combined with gas flux measurements made in 2010 at riparian buffers located in similar HGM settings across the White River watershed (Fisher et al., 2014; Vidon et al., 2014; Jacinthe et al., 2015). For that analysis, gas fluxes were collated for the months April-May 2010 (rainfall: 183 mm; temperature: 17 ^oC) and for the months August-September 2010 (rainfall: 24 mm; temperature: 24 ^oC). These periods were treated as wet and dry seasons respectively in the analysis. Results showed (Tables 7 and 8) that, in almost all cases and irrespective of the season, HGM setting was a significant controlling factor of GHG emission. Consistent with the 2011 gas flux measurements, the 2010 data showed significantly higher CO_2 emission from the HGM-1 buffers and more intense N_2O efflux during the wet season from the HGM-3 buffers. Similar to the 2011 results (Fig. 4), the HGM-2 units were the lowest N_2O emitters and also showed the highest capacity to consume CH_4, especially during the dry season (Table 7).

4. Discussion

Several past studies have characterized riparian buffers on the basis of fluvial landforms and hydrologic connectivity with adjacent channels (Nanson and Croke, 1992; Baker and Wiley, 2004; Rinaldi et al., 2016). These studies have almost exclusively focused on vegetation community composition, density and diversity as the integrated expression of the interactions between a given river system and its floodplains (Nanson and Croke, 1992; Bendix and Hupp, 2000; Baker and Wiley, 2004; Goebel et al., 2006; Rinaldi et al., 2016). To our knowledge, there has been no systematic attempt at linking GHG dynamics and riparian landforms. The present study was designed to investigate whether such linkages exist, and whether the intensity of GHG fluxes in riparian buffers varies in a predictable manner depending on their hydro-geomorphological location. The study results indicate that the HGM-defined riparian buffers are noticeably distinct with regard to soil properties (Tables 2-4), and fluxes of the GHG species monitored in the present study (Tables 5 and 8; Figs. 2-4 and Fig. 6). Overall, the HGM-1 buffers are strong CO_2 emitters whether in wet or dry period, the HGM-2 buffers act as strong CH_4 sinks, whereas N_2O fluxes are higher and more variable at the HGM-3 than at the other types of riparian buffers investigated (Tables 5). A similar trend was observed (Tables 7 and 8) in prior investigations conducted at comparable riparian sites in the White River watershed (Fisher et al, 2014; Jacinthe et al., 2015).

4.1. Hydrobiogeochemical controls on GHG emissions

Soil moisture and temperature are common regulators of CO_2 efflux from soils. In the temperate humid region, soil temperature is often the controlling factor of CO_2 emission whereas soil moisture is often the determining factor in arid environments (McLain and Martens, 2006).

Thus, the correlation (Table 6) between soil moisture and CO_2 flux during the dry season suggests that soil microbial activity at the study sites was severely water-limited during that period, which is consistent with the exceptionally low precipitation amount in July-August 2011 (40 mm as opposed to 195 mm normally). Of the riparian sites investigated, the HGM-1 types are protected from flooding; yet, they emitted significantly more CO_2 than the other buffers (Tables 5, 7 and 8). This observation is in contrast with the results of Samaritani et al. (2011) who reported higher rates of CO_2 emission in riparian buffers along flood-affected compared to non-flooded sections of the Thur River (Switzerland). Previous work at riparian sites in the White River watershed has also shown an increase in CO_2 flux with increased flood frequency (Jacinthe, 2015). Therefore, higher CO_2 emission at the HGM-1 sites likely reflects differences among sites in soil C quality as suggested by the amount of extractable DOC, C/N ratio of soil organic matter and laboratory assays of soil respiration (Table 2).

Methane fluxes at the land surface is the balance between CH_4 biological production and consumption as CH_4 diffuses from its zone of production. Methanogenesis is controlled by soil moisture, soil redox status, temperature and organic substrates to support microbial activity (indirectly creates O_2-depleted pockets). In the present study, significant relationships between these variables and CH_4 fluxes, especially during the wet season (Table 6), suggest that CH_4 production was likely non negligible during that period, although occurring at lower rates than CH_4 consumption activity. In riparian buffers where a high water table occurs and intersects the upper soil layers, vigorous emission of CH_4 has been documented (Van den Pol-Van Dasselaar et al., 1998; Vilain et al., 2010). Although water table depth was not monitored and evidence of ponding water not found, the near-surface soil layers at the riparian sites were probably wet enough to harbor centers of methanogenic activity. Conversely, a significant increase in CH_4

uptake was observed during the dry season (Fig. 3; Tables 5 and 7). Averaged over all the sampling sites, the rate of CH_4 uptake doubled during the dry season (-0.68 mg CH_4-C m^{-2} d^{-1}) compared to the wet season (-0.31 mg CH_4-C m^{-2} d^{-1}). Consistent with the HGM by season interaction (Tables 5 and 7), the seasonal increase in CH_4 consumption was most pronounced at the HGM-2 sites. The seasonal increase in CH_4 uptake was positively related to soil sand content, suggesting that in the dry season CH_4 flux was predominantly controlled by methanotrophy, a diffusion-dependent process likely facilitated by coarse soil texture as long as soil moisture remains above a certain threshold. For the McCloud (#6) and Bargersville (#9) sites (Table 2, Figs. 1 and 3), the seasonal increase in CH_4 consumption was much less than soil sand content would predict. At these sites, dry season CH_4 uptake was probably limited by low soil moisture (< 0.14 g H_2O g^{-1} soil). The sensitivity of methanotrophs to soil moisture stress is well known (Gulledge and Schimel, 1998; Van den Pol-Van Dasselaar et al., 1998). Research has shown that CH_4 uptake in soils occurs at an optimum soil moisture between 0.20 and 0.35 g H_2O g^{-1} soil, and that the process can be halted when soil moisture falls below 0.05 g H_2O g^{-1} soil (Van den Pol-Van Dasselaar et al., 1998). Therefore, unfavorable conditions for the methanotrophs due to extremely low soil moisture at these two sites may have contributed to the low rate of CH_4 uptake observed during the dry season sampling.

The strong correlation (r^2: 0.83) between N_2O fluxes and soil NO_3^- during the wet season was expected, and similar relationships were reported for various ecosystems such as croplands, grassland, and forests (Vilain et al., 2010). During the wet season sampling period, soils were relatively warm (17.9±2.5 ^oC) and moist (0.28±0.09 g H_2O g^{-1} soil); therefore, N_2O production likely originated from soil denitrification and was largely dependent on NO_3^-availability. Taking an average bulk density of 1.1 g cm^{-3} for the region's riparian soils (Jacinthe et al., 2012; Fisher

et al., 2014), water-filled pore space (WFPS) would be 61% on average, barely within the WFPS threshold of 60-70% above which maximum rates of N_2O emission have typically been observed (Vilain et al., 2010). Therefore, even during the wet season, the N_2O fluxes measured in this study most likely do not represent the maximum emission at the study sites. In fact, in previous investigations in the same watershed and at sites similar to the HGM-3 riparian buffers, N_2O fluxes as high as 28 mg N_2O-N m^{-2} d^{-1} (Fisher at al., 2014; WFPS: 72%) and 81 mg N_2O-N m^{-2} d^{-1} (Jacinthe et al., 2012; WFPS> 100%) were measured following flood events. These levels of emission are several-fold greater than the highest N_2O emission rate (4.51 mg N_2O-N m^{-2} d^{-1}) measured in the present study. In the dry season, N_2O emission was likely limited by both low soil NO_3^- (5.7±3.0 mg N kg^{-1} soil) and soil moisture content (0.19±0.09 g H_2O g^{-1} soil) (Tables 3 and 4). Instead, during that period, N_2O flux was related to soil NH_4^+ concentration and soil respiration, suggesting that N_2O production was associated with mineralization of soil organic matter and nitrification (Mummey et al., 1994).

In addition to surface processes, fluctuation in the riparian groundwater level may have also contributed to differences among the riparian sites with respect to N_2O fluxes (ranking: HGM-3 > HGM-1 > HGM-2; Tables 5 and 7). That ranking was not, however, totally consistent with the DEA results (HGM-1 > HGM-3 > HGM-2; Tables 2). A previous investigation (Liu et al., 2014) conducted at riparian sites similar to those selected for the present work has reported higher mass flux of NO_3^- removal (9.4-21.7 versus 0.4-1.9 mg N day^{-1} m^{-1}) at HGM-3 than at HGM-1 sites. That investigation (Liu et al., 2014) also showed greater fluctuations in water table depth at HGM-3 (from 240 cm below ground surface to 215 cm above ground) than at HGM-1 sites (between 20 and 190 cm bgs). Therefore, limited interaction between groundwater and the biologically-active surface soil layers at the HGM-1 buffers likely contributed to the lower N_2O

fluxes despite the much higher denitrification potential of these soils (Table 2). The relative stability of groundwater level at HGM-1 likely results from the presence of subsurface tile drain systems that run underneath most HGM-1 buffers in this physiographic region. As noted previously, subsurface tile drainage, facilitates the removal of excess water from poorly-drained soils and allows timely implementation of farming activities. Subsurface drainage is very common in US Midwest agricultural landscapes (present in 35-50% of all croplands in Ohio, Indiana and Illinois; NRCS, 1987). While these hydrological alterations may result in low N_2O emission, they can also lead to inefficient nutrient retention in riparian buffers and worsening water quality problems (Jacinthe et al., 2015).

4.2. Riparian HGM characteristics as a tool to estimate GHG emissions

Although relationships were found between GHG fluxes and soil temperature (ex. CH_4), soil moisture (CH_4 in wet season, CO_2 in dry season), and other intrinsic soil properties, the relative significance of these relationships varied with season and for each gas species (Table 6). This variability makes it difficult to use these relationships to scale up GHG fluxes at the watershed scale. In addition, these soil and environmental variables are not widely available at the landscape scale and must be measured, further raising questions about the accuracy and cost-effectiveness of regional GHG inventories that are based on these variables.

Overall, our results (Tables 7 and 8; Fig. 6) suggest that riparian HGM classes may be a reasonable approach to categorize the range of GHG emission rates in riparian zones in a region. As indicated previously, riparian ecosystems are often classified on the basis of vegetation cover (Palik et al., 2004; Goebel et al., 2006). However, vegetation cover based classifications generally fail to predict key riparian functions such as NO_3^- removal in the subsurface (see

Dosskey et al., 2010). As Clement et al. (2002) argued, divergent results in terms of the role of vegetation on NO_3^- removal in riparian zones could be due to the failure to account for differences in hydrogeomorphic settings among study sites. Results of the present study, along with those of previous investigations in the White River watershed (Jacinthe et al., 2012; Fisher et al., 2014; Vidon et al., 2014; Jacinthe et al., 2015) support the idea that one needs to account for HGM settings in order to project riparian functions, and especially GHG emission rates. Although the riparian buffers were distinct in terms of GHG dynamics, the overlap between HGM-2 and HGM-3 shown by DCA (Fig 6) is an observation that deserves further consideration. This observation might suggest that the number of sites (3 per HGM type) was inadequate to fully characterize these classes of riparian buffers. It might also be an indication that the HGM classification developed for the White River watershed (Panunto, 2012) needs some refinement through perhaps the inclusion of sub-units within the larger group of HGM-2 and HGM-3 riparian buffers.

More broadly speaking, these findings are also consistent with research stressing the relationship between landscape HGM characteristics and riparian functions, and with our current understanding of the impact of topography, surficial geology, and soil types on riparian biogeochemical processes (Gold et al., 2001; Vidon and Hill, 2004). Riparian landscapes are the product of the interactions of hydrologic and geomorphologic processes that determine the extent of the connection between riparian buffer and adjacent channels. Landscape topography can affect the spatial distribution of soil moisture, nutrient and organic matter within a riparian buffer and, consequently the intensity of GHG emission in different landscape positions. Past studies (Dhondt et al., 2004; Vilain et al., 2010) have documented relationships between NO_3^- removal, N_2O production and landscape characteristics of riparian buffers. Work in southern Ontario

(Vidon and Hill, 2004) has shown that slope gradient and configuration (concave, convex) at the upland-riparian zone margin determines water table position, and ultimately the NO_3 removal capacity of riparian buffers. The present investigation extends that conceptual understanding of local relationships between landscape features and riparian functions, and demonstrates that channel gradient, for example, could be a good predictor of N_2O flux in riparian buffers. In addition, our results have shown consistent differences among the types of riparian sites with respect to GHG fluxes (two consecutive years; Tables 5 and 7). These findings suggest that the upscaling of riparian zone GHG data can be greatly facilitated if the selection of field studies is guided by hydro-geomorphic criteria. Therefore, the HGM classification could emerge as a fruitful approach for functional characterization of soil processes and trace gas dynamics in riparian buffers in the US Midwest, and perhaps in other eco-regions. Increased availability of satellite and airborne remote sensing information (e.g. LiDAR, light detection and ranging) and other fine-scale digital landscape data should improve our ability to map/classify riparian buffers and generate regional-scale estimates of riparian GHG emission.

5. ACKNOWLEDGEMENTS

This work was supported by USDA-AFRI grant 2009-35112-05241. Authors thank the landowners and park managers for granting access to the study sites. Authors thank Lori Bebinger, Katelin Fisher, Xiaoqiang Liu, Charlotte Mason, and Lauren Thomas for field and laboratory assistance.

6. References

Addy, K.L., Gold, A.J., Groffman, P.M., Jacinthe, P.A., 1999. Ground water nitrate removal in

subsoil of forested and mowed riparian buffer zones. J. Environ. Qual. 28, 962-970.

Antevs, E. 1929. Maps of the Pleistocene glaciations. Bull. Geol. Soc. Am. 40, 631-720.

Audet, J., Elsgaard, L., Kjaergaard, C., Larsen, S.E., Hoffmann, C.C., 2013. Greenhouse gas emissions from a Danish riparian wetland before and after restoration. Ecol. Eng. 57, 70-182.

Baker, M.E., Wiley, M.J., 2004. Characterization of woody species distribution in riparian forests of lower Michigan, USA using map-based models. Wetlands 24, 550-561.

Bedient, P.B., Huber, W.C., Vieux, B.C., 2007. Hydrology and Floodplain Analysis, 4th edition. Prentice Hall, London, 795 p.

Bendix, J., Hupp, C.R., 2000. Hydrological and geomorphological impacts on riparian plant communities. Hydrol. Process. 14, 2977-2990.

Clément, J.C., Pinay, G., Marmonier, P., 2002. Seasonal dynamics of denitrification along topohydrosequences in three different riparian wetlands. J. Environ. Qual. 31, 1025-1037.

Couwenberg, J., Thiele, A., Tanneberger, F., Augustin, J., Bärisch, S., Dubovik, D., Liashchynskaya, N., Michaelis, D., Minke, M., Skuratovich, A., Joosten, H., 2011. Assessing greenhouse gas emissions from peatlands using vegetation as a proxy. Hydrobiologia 674, 67-89.

Dhondt, K., Boeckx, P., Hofman G., Van Cleemput, O., 2004. Temporal and spatial patterns of denitrification enzyme activity and nitrous oxide fluxes in three adjacent vegetated riparian buffer zones. Biol. Fert. Soils 40, 243-251.

Dias, A.T.C., Hoorens, B., Van Logtestijn, R.S.P. Vermaat, J.E., Aerts, R., 2010. Plant species composition can be used as a proxy to predict methane emissions in peatland ecosystems after land-use changes. Ecosystems 13, 526-538.

Dosskey, M.G., Vidon, P., Gurwick, N.P., Allan, C.J., Duval, T., Lowrance, R., 2010. The role of riparian vegetation in protecting and improving chemical water quality in streams. J. Am. Water Resour. Assoc. 46, 261-277.

Fisher, K., Jacinthe, P.A., Vidon, P., Liu, X., Baker, M.E., 2014. Nitrous oxide emission from cropland and adjacent riparian buffers in contrasting hydrogeomorphic settings. J. Environ. Qual. 43, 338-348.

Franzmeier, D.P., Kladivko, E.J., 2001. Drainage and Wet Soil Management: Wet Soils of Indiana. Purdue Extension Publ. AY-301. Purdue University Cooperative Extension Service, West Lafayette, Indiana.

Goebel, P.C., Pregitzer, K.S., Palik, B.J., 2006. Landscape hierarchies influence riparian ground-flora communities in Wisconsin, USA. For. Ecol. Manage. 230, 43-54.

Gold, A.J., Groffman, P.M., Addy, K., Kellog, D.Q., Stolt, M., Rosenblatt, A.E., 2001. Landscape attributes as controls on ground water nitrate removal capacity of riparian zones. J. Am. Water Resour. Assoc. 37, 1457-1464.

Gulledge, J., Schimel, J.P., 1998. Moisture control over atmospheric methane consumption and CO_2 production in diverse Alaskan soils. Soil Biol. Biochem. 30, 1127-1132.

Hammer, O., Harper, D.A.T, Ryan, P.D., 2001. PAST: Paleontological Statistics Software Package for Education and Data Analysis. Palaeontologia Electronica 4, art. 4: 9 pp., http://palaeo-electronica.org/ 2001_1/past/issue1_01.htm.

Hefting, M.M., Bobbink R., de Caluwe, H., 2003. Nitrous oxide emission and denitrification in chronically nitrate-loaded riparian buffer zones. J. Environ. Qual. 32, 1194-1203.

Hopfensperger, K.N., Gault, C.M., Groffman, P.M., 2009. Influence of plant communities and

soil properties on trace gas fluxes in riparian northern hardwood forests. For. Ecol. Manage. 258, 2076-2082.

IPCC, 2013. Climate Change 2013: The Physical Science Basis. Contribution of Working Group I to the Fifth Assessment Report of the Intergovernmental Panel on Climate Change. Cambridge University Press, Cambridge, UK.

Jacinthe, P.A., Groffman, P.M., Gold, A.J., Mosier, A., 1998. Patchiness in microbial nitrogen transformations in groundwater in a riparian forest. J. Environ. Qual. 27, 156-164.

Jacinthe, P.A., Bills, J.S., Tedesco, L.P., Barr, R.C., 2012. Nitrous oxide emission from riparian buffers in relation to vegetation and flood frequency. J. Environ. Qual. 41, 95-105.

Jacinthe, P.A., 2015. Carbon dioxide and methane fluxes in variably-flooded riparian forests. Geoderma 241, 41-50.

Jacinthe, P.A., Vidon, P., Fisher, K., Liu, X., Baker, M.E., 2015. Soil methane and carbon dioxide fluxes from cropland and riparian buffers in different hydrogeomorphic settings. J. Environ. Qual. 44, 1080-1090.

Kim, D.G., Isenhart, T.M., Parkin, T.B., Schultz, R.C., Loynachan, T.E., 2010. Methane flux in cropland and adjacent riparian buffers with different vegetation covers. J. Environ. Qual. 39, 97-105.

Liu, X., Vidon, P., Jacinthe, P.A., Fisher, K., Baker, M.E., 2014. Seasonal and geomorphic controls on N and P removal in riparian zones of the US Midwest. Biogeochemistry 119, 245-257.

McLain, J.E.T., Martens, D.A., 2006. Moisture controls on trace gas fluxes in semiarid riparian soils. Soil Sci. Soc. Am. J. 70, 367-377.

Mummey, D.L., Smith, J.L., Bolton, H., 1994. Nitrous oxide flux from a shrub-steppe

ecosystem: sources and regulation. Soil Biol. Biochem. 26, 279-286.

Nanson, G.C., Croke, J.C., 1992. A genetic classification of floodplains. Geomorphology 4, 459-486.

NRCS, 1987. Farm Drainage in the United States: History, Status and Prospects. Misc. Publ. No. 1455. United States Department of Agriculture (USDA) Natural Resources Conservation Service (NRCS), Washington, DC.

Palik, B., Tang, S.M., Chavez, Q., 2004. Estimating riparian area extent and land use in the Midwest. Gen. Tech. Rep. NC-248. USDA, Forest Service, North Central Research Station, St. Paul, MN.

Panunto, M.H. 2012. Effects of river valley segment sequencing on floodplain hydroperiods. University of Maryland at Baltimore County (UMBC). MS Thesis.

Rinaldi, M., Gurnell, A.M., del Tánago, M.G., Bussettini, M., 2016. Classification of river morphology and hydrology to support management and restoration. Aquat. Sci. 78, 17-33.

Samaritani, E., Shrestha, J., Fournier, B., Frossard, E., Gillet, F., Guenat, C., Niklaus, P.A., Pasquale, N., Tockner, K., Mitchell, E.A.D., Luster, J., 2011. Heterogeneity of soil carbon pools and fluxes in a channelized and a restored floodplain section (Thur River, Switzerland). Hydrol. Earth Syst. Sci. 15, 1757-1769.

Smith, M.S., Tiedje, J.M., 1979. Phases of denitrification following oxygen depletion in soil. Soil Biol. Biochem. 11, 261-267.

Van den Pol-Van Dasselaar, A., Van Beusichem M.L., Onema, O., 1998. Effects of soil moisture content and temperature on methane uptake by grasslands on sandy soils. Plant Soil 204, 213-222.

Van Haren, J.L.M., de Oliveira, R.C., Restrepo-Coupe, N., Hutyra, L., de Camargo, P.B.Keller, M., Saleska, S.R., 2010. Do plant species influence soil CO_2 and N_2O fluxes in a diverse tropical forest? J. Geophys. Res. 115, G03010.

Vidon, P., Hill, A.R., 2004. Landscape controls on nitrate removal in stream riparian zones. Water Resour. Res. 40, W03201.

Vidon, P., Jacinthe, P.A., Liu, X, Fisher, K., Baker, M.E. 2014. Hydrobiogeochemical controls on riparian nutrient and greenhouse gas dynamics: 10 years post-restoration. J. Am. Water Resour. Assoc. 50, 639-652.

Vilain, G., Garnier, J., Tallec, G., Cellier, P., 2010 Effect of slope position and land use on nitrous oxide (N_2O) emissions (Seine Basin, France). Agric. For. Meteorol. 150, 1192-1202.

Walker, J.T. Geron, C.D., Vose, J.M., Swank, W.T., 2002. Nitrogen trace gas emissions from a riparian ecosystem in southern Appalachia. Chemosphere 49, 1389-1398.

Woltemade, C.J., Potter K.W., 1994. A watershed modeling analysis of fluvial geomorphologic influences on flood peak attenuation. Water Resour. Res. 30, 1933-1942.

Zimmer, M.A., Lautz, L.K., 2013. Temporal and spatial response of hyporheic zone geochemistry to a storm event. Hydrol. Process. 28, 2324-2337.

Figure captions

Fig. 1. The White River watershed in Indiana (depicted by the gray area in the Indiana map insert, top left). The circles indicate locations of the study sites along the main stem (3^{rd} - 4^{th} order) and tributaries (1^{st} - 2^{nd} order) of White River. The sites sampled in 2010 are indicated by a triangle. The number in parentheses corresponds to site number (listed in Table 1). Shown in the bottom right insert are sketches (not to scale) depicting landforms associated with the three types of riparian buffers investigated.

Fig. 2. Seasonal variation in daily fluxes of carbon dioxide at nine riparian sites in the White River watershed. Spatial variability of fluxes at each site is shown in the box plot. The filled circle and the horizontal bar in each box represent the mean and median flux, respectively.

Fig. 3. Seasonal variation in daily fluxes of methane at nine riparian sites in the White River watershed. Spatial variability of fluxes at each site is shown in the box plot. The filled circle and the horizontal bar in each box represent the mean and median flux, respectively.

Fig. 4. Seasonal variation in daily fluxes of nitrous oxide at nine riparian sites in the White River watershed. Spatial variability of fluxes at each site is shown in the box plot. The filled circle and the horizontal bar in each box represent the mean and median flux, respectively.

Fig. 5. Relationships of soil nitrate concentration (left) and adjacent channel gradient (right) with nitrous oxide flux in riparian buffers during the wet season.

Fig. 6. Scatter plots of discriminant analysis (DCA) scores showing separation among types of riparian buffers (HGM-1, HGM-2, and HGM-3) on the basis of greenhouse gas (CO_2, CH_4, and N_2O) fluxes. Group centroids are shown in the graph insert (error bars represent one standard deviation).

Fig 1

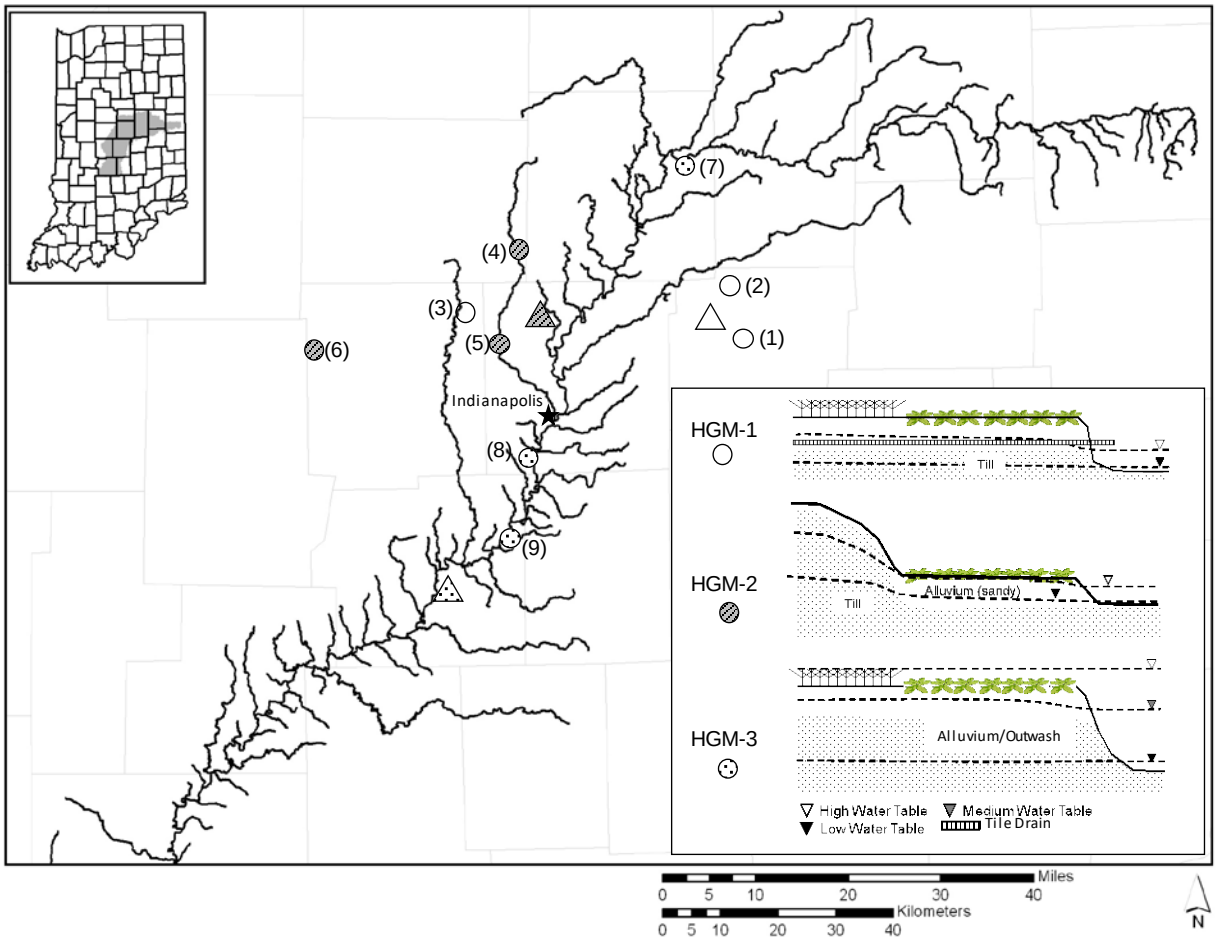
(1)
(2)
(3)
(4)
(5)
(6)
(7)
(8)
(9)
Indianapolis
HGM-1
Till
HGM-2
Alluvium (sandy)
Till
HGM-3
Alluvium/Outwash
High Water Table
Medium Water Table
Low Water Table
Tile Drain
Miles
0 5 10 20 30 40
Kilometers
0 5 10 20 30 40
N

Fig 2

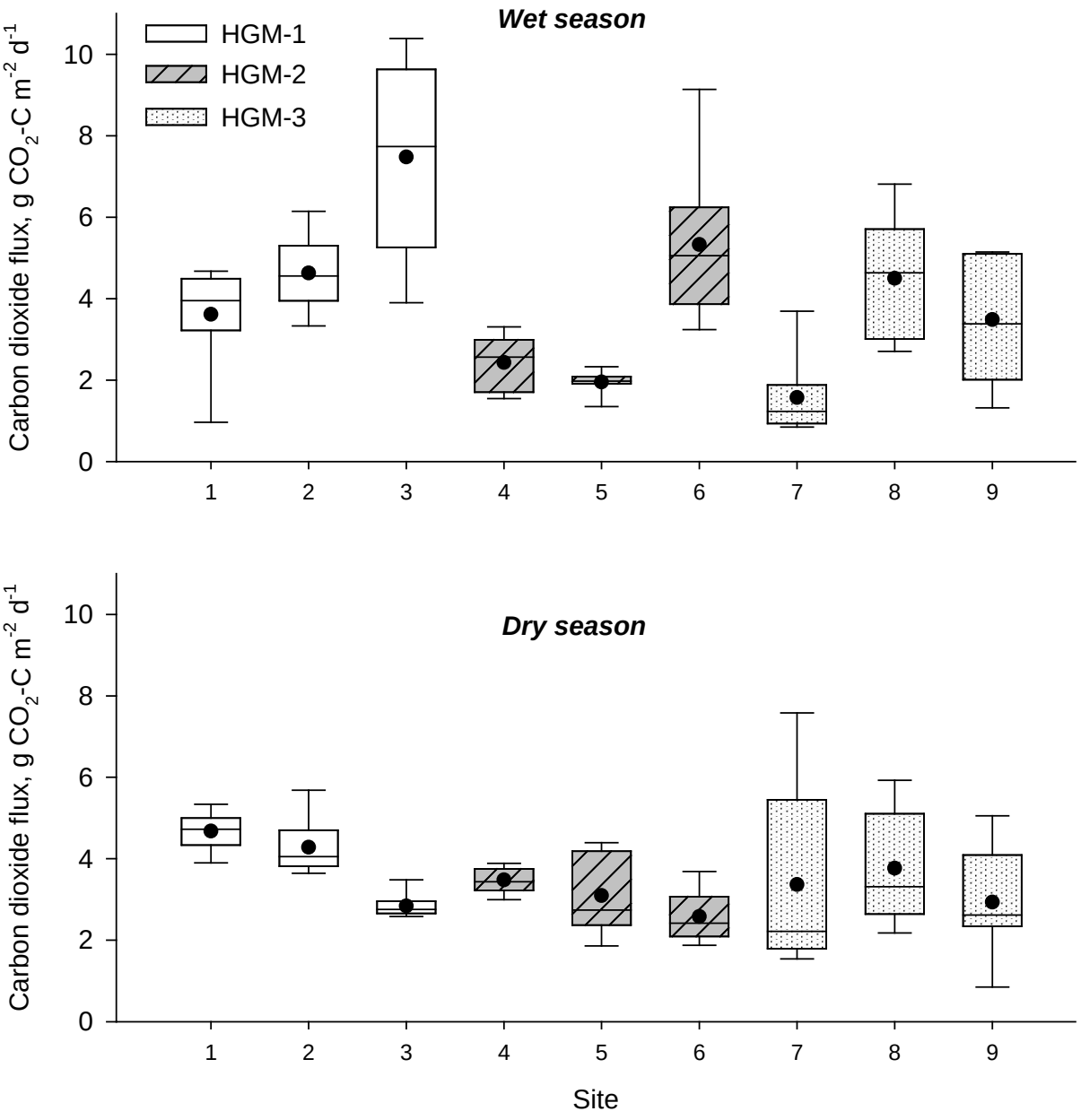
Wet season
HGM-1
HGM-2
HGM-3
Carbon dioxide flux, g CO2-C m-2 d-1
0
2
4
6
8
10
1
2
3
4
5
6
7
8
9
Dry season
Carbon dioxide flux, g CO2-C m-2 d-1
Site

Fig 3

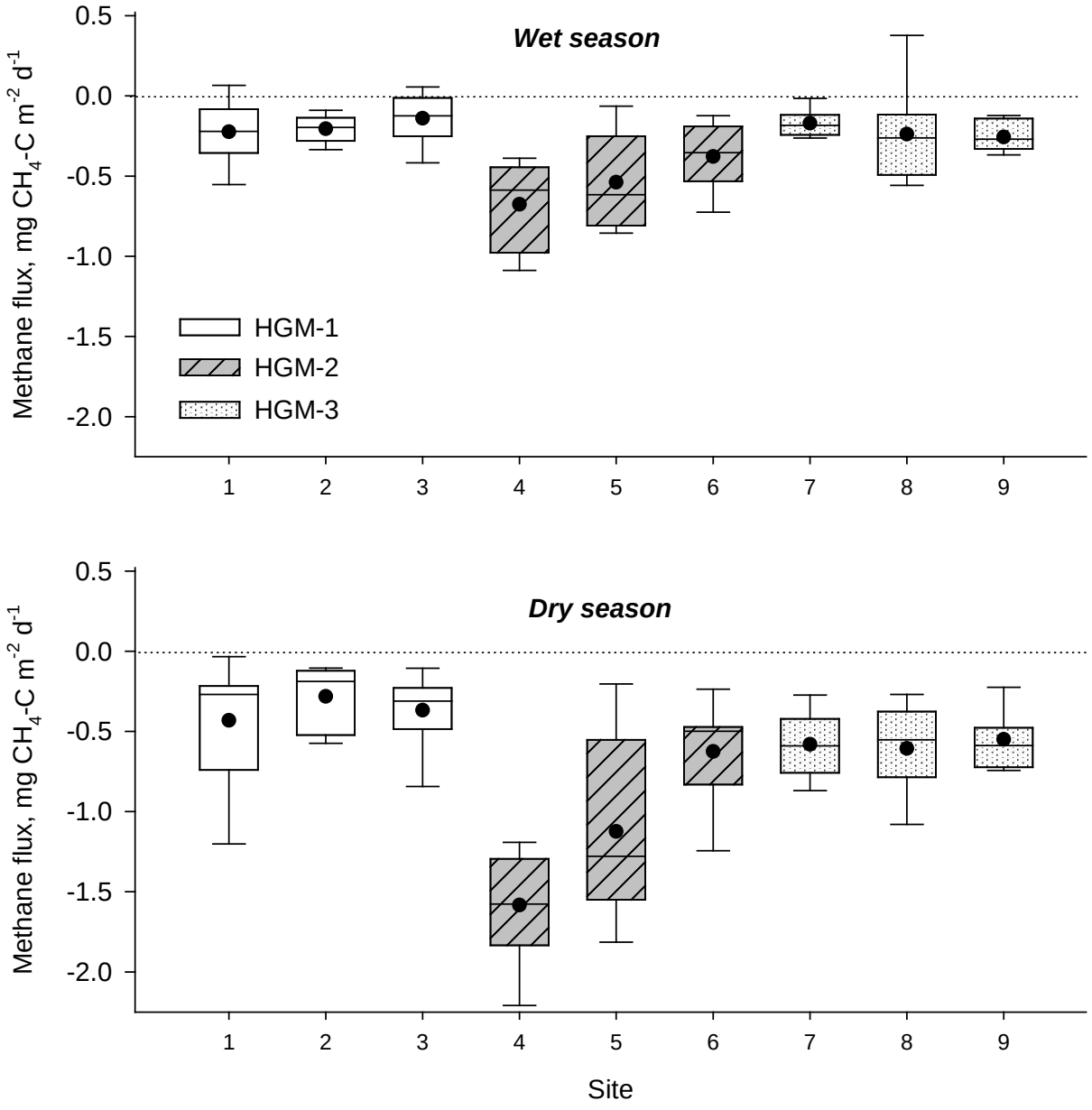
Wet season
Dry season
Methane flux, mg CH4-C m-2 d-1
0.5
0.0
-0.5
-1.0
-1.5
-2.0
HGM-1
HGM-2
HGM-3
1
2
3
4
5
6
7
8
9
Site

Fig 4

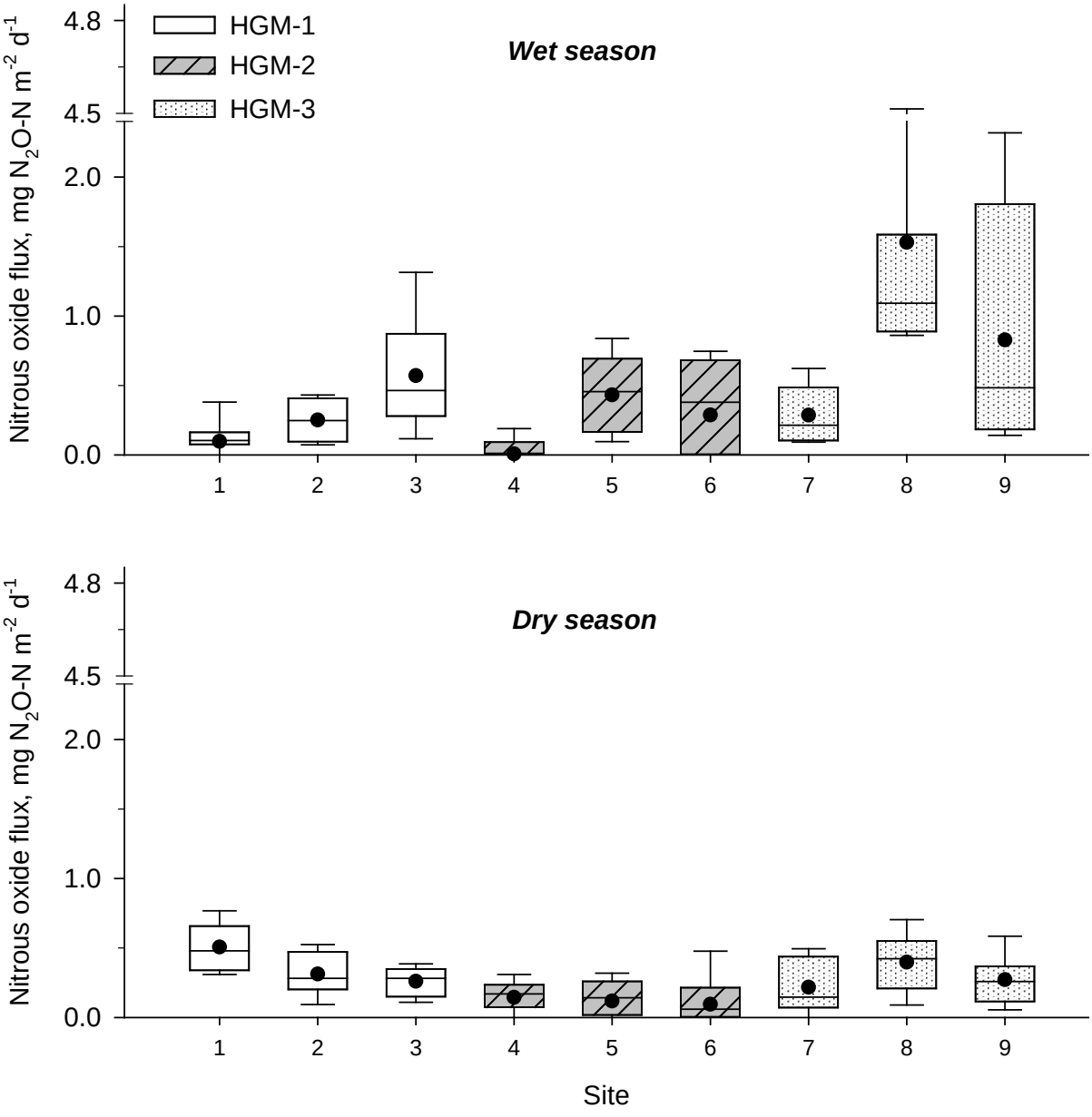
HGM-1
HGM-2
HGM-3
Wet season
Dry season
Nitrous oxide flux, mg N2O-N m-2 d-1
4.8
4.5
2.0
1.0
0.0
1
2
3
4
5
6
7
8
9
Site

Fig 5

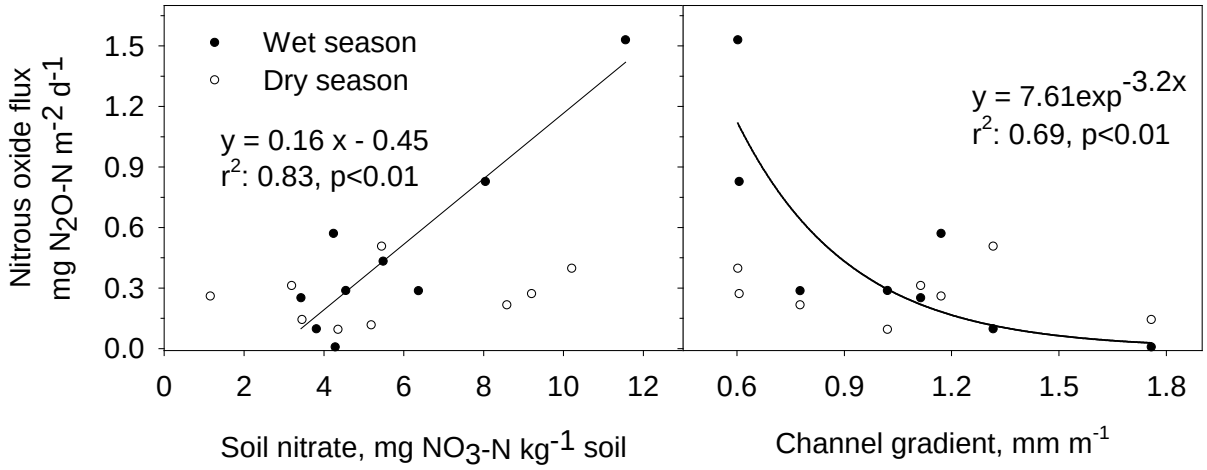
Nitrous oxide flux
mg N2O-N m-2 d-1
Wet season
Dry season
y = 0.16 x - 0.45
r2: 0.83, p<0.01
y = 7.61exp-3.2x
r2: 0.69, p<0.01
Soil nitrate, mg NO3-N kg-1 soil
Channel gradient, mm m-1

Fig 6

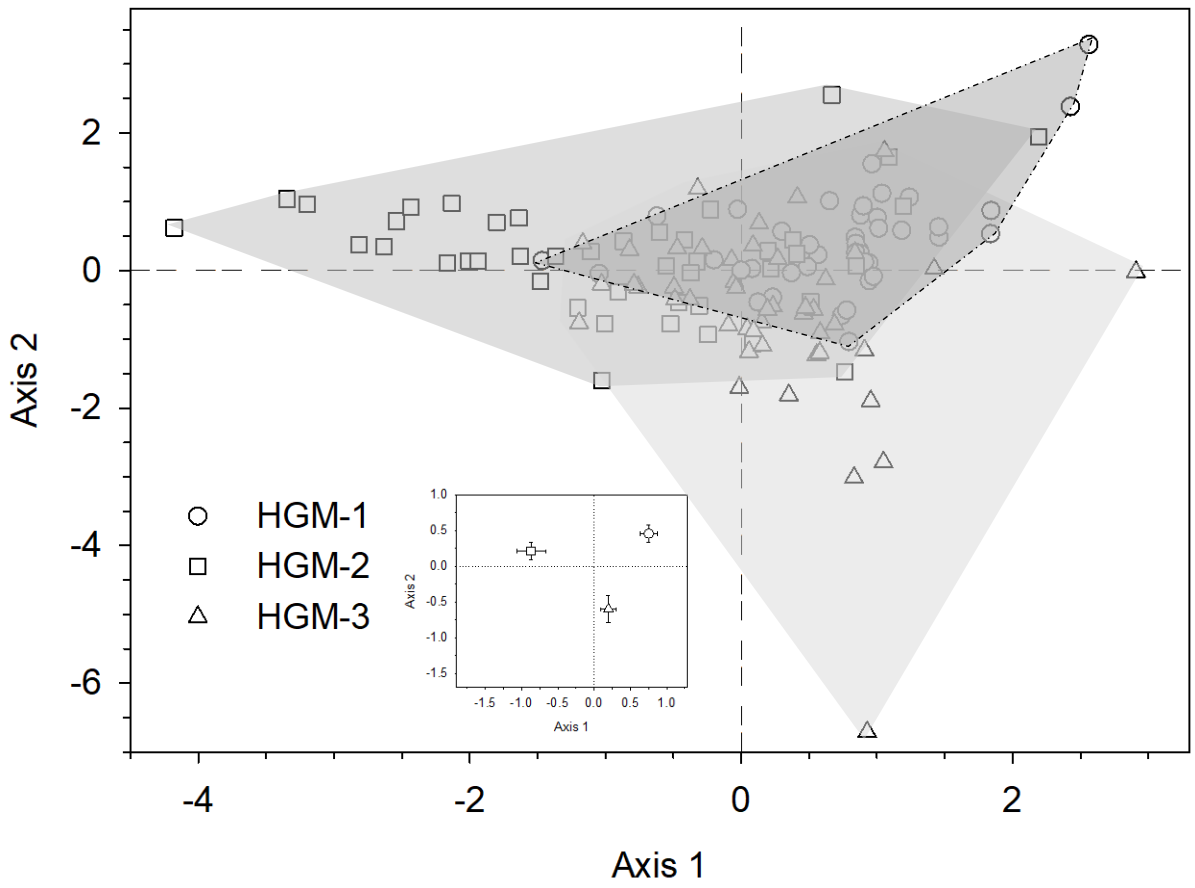
Axis 2
Axis 1
HGM-1
HGM-2
HGM-3
2
0
-2
-4
-6
-4
-2
0
2
Axis 2
Axis 1
1.0
0.5
0.0
-0.5
-1.0
-1.5
-1.5
-1.0
-0.5
0.0
0.5
1.0

Table 1
Location of the study sites selected to represent the three major riparian hydro-geomorphic units (HGM) in the
IN.

Class	Site	Name	Adjacent stream	Coordinates	Drainage area (10^3 km^2)	Chan (r
HGM-1[a]	1	LWD-2 [b]	Leary Weber Ditch	39° 51' 27" N, 85° 50' 31"W	0.2	
	2	LWD-3	Leary Weber Ditch	39° 51' 16" N, 85° 50' 22" W	0.3	
	3	Hessian	School Branch	39° 53' 38" N, 86° 21' 4" W	0.8	
HGM-2	4	Rice estate	Fishback Creek	39° 53' 16" N, 86°19' 6" W	5.3	
	5	Hideaway	Eagle Crest Branch	39° 52' 22" N, 86°18' 54" W	0.2	
	6	McCloud	Big Walnut Creek	39° 49' 56" N, 86° 41' 6" W	30.9	
HGM-3	7	Strawtown	White River	40° 7' 35" N, 85° 56' 51" W	185.6	
	8	Southwestway	White River	39° 39' 23" N, 86° 14' 9" W	503.5	
	9	Bargersville	White River	39° 36' 7" N, 86° 14' 33" W	517.7	

[a] Class of riparian buffers are determined by hydro-geomorphic settings. The channel adjacent to HGM-1 ripari
periodically dredged and deepened to prevent flooding of nearby agricultural fields. Sites 1-4 are adjacent to ac
agricultural fields, sites 5-9 are located within protected areas (parks, nature reserves).
[b] Abbreviation: Leary Weber ditch (LWD).
[c] Obtained from StreamStats (http://water.usgs.gov/osw/streamstats/indiana.html). Along the main stem of the W
9), a mean channel gradient of 0.77 and 0.49 mm m^{-1} was derived from a regional landscape analysis for stream
south of Indianapolis, respectively [21].

Table 2.

General properties of riparian soil (0-20 cm) in different hydro-geomorphic (HGM) settings in the White River are means of 8-9 sampling points per site with standard deviation in parentheses.

Riparian class	Site #	Site name	Soil properties					
			pH	Texture	Organic C, g C kg^{-1}	Total N, g N kg^{-1}	DOC, mg C kg^{-1}	BSI µg C g
HGM-1[a]	1	LWD-2[b]	7.3 (0.1)	CL [38, 28][c]	43.2 (5.5)	2.1 (0.6)	55.6 (3.7)	0.21 (
	2	LWD-3	7.1 (0.2)	CL [33, 27]	39.3 (2.3)	1.7 (0.4)	116.6 (11)	0.31 (
	3	Hessian	5.9 (0.2)	CL [41, 30]	37.2 (0.7)	1.9 (0.1)	55.7 (10.3)	0.28 (
	Riparian class average		6.8		40.3 B[d]	1.9	73.1 A	0.26
HGM-2	4	Rice estate	7.2 (0.1)	SCL [48, 25]	35.8 (3.1)	1.8 (0.3)	13 (4.6)	0.11 (
	5	Hideaway	7.3 (0)	SL [54, 8]	32.1 (4.3)	1.3 (0.4)	16.7 (4.7)	0.12 (
	6	McCloud	7.3 (0.1)	SL [56, 14]	33.5 (2)	1.7 (0.2)	11.7 (5.6)	0.08 (
	Riparian class average		7.3		33.9 C	1.6	13.5 C	0.10
HGM-3	7	Strawtown	7.2 (0.1)	L [31, 23]	48.3 (6.2)	1.9 (0.3)	48.2 (15.5)	0.12 (
	8	SWW	7.2 (0.1)	SCL [48, 27]	49.4 (1.2)	1.7 (0.3)	57.3 (22.2)	0.13 (
	9	Bargersville	7.1 (0.1)	SCL [52, 21]	46.9 (3.3)	1.7 (0.2)	57.2 (2.8)	0.12 (
	Riparian class average		7.2		47.9 A	1.7	54.8 B	0.12

[a] Class of riparian buffers as determined by hydro-geomorphic setting.

[b] LWD: Leary Weber ditch; SWW: Southwestway park; L: loam; CL: clay loam; SL: sandy loam; SCL: sandy c dissolved organic carbon; BSR: basal soil respiration; DEA: denitrification enzyme activity.

[c] Numbers in brackets are the % sand and clay, respectively.

[d] For a given soil property, mean values in the same column followed by different letters are significantly differ

Table 3.

Seasonal variation in mineral N and dissolved organic carbon (DOC) at the riparian buffers in the White River
are means of 8-9 sampling points per site with standard deviation in parentheses.

Riparian class	Site #	Site name	Wet season			Dry s	
			NO_3, mg N kg^{-1}	NH_4, mg N kg^{-1}	DOC, mg C kg^{-1}	NO_3, mg N kg^{-1}	N mg
HGM-1 [a]	1	LWD-2	3.8 (1.1)	4.8 (1.3)	55.6 (3.7)	5.4 (0.3)	6.5
	2	LWD-3	3.4 (1.4)	4.3 (1.7)	116.6 (11)	3.2 (0.2)	6.7
	3	Hessian	4.2 (2.9)	12.6 (3.8)	55.7 (10.3)	1.2 (0.3)	5.4
	Riparian class average		3.8 B [b]	7 A	73.1 A	3.5 C	6.
HGM-2	4	Rice estate	4.3 (2.7)	5.8 (3.7)	13 (4.6)	3.5 (0.2)	4.8
	5	Hideaway	5.5 (1.8)	1.8 (1)	16.7 (4.7)	5.2 (0.7)	5.7
	6	McCloud	4.5 (2.2)	5 (2.5)	11.7 (5.6)	4.4 (0.6)	4.8
	Riparian class average		4.8 B	4.1 B	13.5 C	4.4 B	5.
HGM-3	7	Strawtown	6.4 (3)	5.9 (2.7)	48.2 (15.5)	8.6 (1.3)	6.4
	8	Southwestway	11.6 (6.9)	5.1 (3)	57.3 (22.2)	10.2 (1.4)	5.1
	9	Bargersville	8 (3.9)	5.1 (2.5)	57.2 (2.8)	9.2 (0.6)	4.6
	Riparian class average		8.7 A	5.4 B	54.8 B	9.3 A	5.

[a] HGM: hydro-geomorphic settings; LWD: Leary Weber ditch.

[b] For a given property, mean values in the same column followed by different letters are significantly different a

Table 4.

Seasonal variation in soil moisture and temperature at the riparian buffers in the White River watershed, IN. Va
sampling points per site with standard deviation in parentheses.

Riparian class	Site #	Site name	Wet season		Dry season	
			Soil moisture, g g^{-1} soil	Temperature, ^{o}C	Soil moisture, g g^{-1} soil	Temperatu ^{o}C
HGM-1[a]	1	LWD-2	0.32 (0.05)	17.3 (1.1)	0.24 (0.02)	23.2 (0.5
	2	LWD-3	0.34 (0.06)	18.7 (1.7)	0.25 (0.03)	23.9 ((0.
	3	Hessian	0.28 (0.11)	17.3 (1.3)	0.18 (0.09)	23.1 (0.4
	Riparian class average		0.31 A[b]	17.7 B	0.23 A	23.4 B
HGM-2	4	Rice estate	0.23 (0.02)	14.7 (0.7)	0.15 (0.01)	22.2 (0.4
	5	Hideaway	0.23 (0.06)	14.5 (0.3)	0.19 (0.04)	22 (0.4)
	6	McCloud	0.22 (0.06)	17.6 (1.0)	0.14 (0.04)	23.2 (0.4
	Riparian class average		0.23 B	15.6 C	0.16 B	22.5 C
HGM-3	7	Strawtown	0.38 (0.07)	19.1 (0.4)	0.24 (0.06)	24.1 (0.2
	8	Southwestway	0.27 (0.11)	20.3 (1.4)	0.16 (0.04)	24.6 (0.6
	9	Bargersville	0.23 (0.07)	21.6 (0.7)	0.13 (0.02)	25.2 (0.3
	Riparian class average		0.29 A	20.3 A	0.17 B	24.6 A

[a] HGM: hydro-geomorphic settings; LWD: Leary Weber ditch.

[b] For a given property, mean values in the same column followed by different letters are significantly different a

Table 5.
Mean greenhouse gas fluxes in riparian buffers as related to hydro-geomorphic (HGM) settings and season (wet period: April-May; dry period: July-August) in 2011. Values are means (standard errors in parentheses) of 40-65 measurements.

		Carbon dioxide ($g\ CO_2\text{-}C\ m^{-2}\ d^{-1}$)	Methane ($mg\ CH_4\text{-}C\ m^{-2}\ d^{-1}$)	Nitrous oxide ($mg\ N_2O\text{-}N\ m^{-2}\ d^{-1}$)
HGM	1	4.54 (0.28) A[a]	-0.28 (0.04) A	0.33 (0.03) B
	2	3.14 (0.21) B	-0.80 (0.08) B	0.17 (0.04) B
	3	3.27 (0.26) B	-0.40 (0.04) A	0.59 (0.11) A
Season	Wet	3.77 (0.26)	-0.32 (0.03) X	0.48 (0.09) X
	Dry	3.44 (0.16)	-0.69 (0.06) Y	0.26 (0.03) Y
Analysis of variance, P>F				
	HGM	<0.001	<0.001	<0.001
	Season	0.21	<0.001	0.02
HGM x season		0.19	0.02	0.04

[a] For a given factor, values in a column followed by different letters are significantly different at $P< 0.05$.

Table 6.
Regression coefficients for the relationships between gas fluxes and soil properties at the riparian sites during the wet and dry seasons.

	Wet season			Dry season		
	CO_2	CH_4	N_2O	CO_2	CH_4	N_2O
Sand	ns	ns	ns	ns	ns	ns
Clay	ns	ns	ns	ns	ns	0.49*
Soil temperature	ns	0.51*	ns	ns	0.36*	ns
Soil moisture	ns	0.42*	ns	0.47*	ns	ns
NH_4^+ concentration	0.48*	ns	ns	0.49*	ns	0.38*
NO_3^- concentration	ns	ns	0.83**	ns	ns	ns
DOC concentration	ns	0.47*	ns	ns	0.43*	ns
Soil organic C	ns	0.43*	ns	ns	ns	ns
C/N ratio	ns	ns	0.55*	ns	ns	ns
Respiration	ns	ns	ns	ns	ns	0.53*
Denitrification activity	ns	0.51*	ns	ns	0.42*	ns

*, **: Statistically significant at $P < 0.05$ and $P < 0.01$, respectively. ns: not statistically significant.

Table 7.
Seasonal variation in greenhouse gas fluxes measured in 2010 in riparian buffers located in different hydro-geomorphic (HGM) settings across the White River watershed, IN. Data are from Vidon et al. (2014) for the SS site, and from Fisher et al. (2014) and Jacinthe et al. (2015) for the other sites. Fluxes are in units: g CO_2-C m^{-2} d^{-1}, mg CH_4-C m^{-2} d^{-1}, and mg N_2O-N m^{-2} d^{-1}. For a given site, the dataset includes 21-30 observations during the wet season, and 18-23 observations during the dry season. Abbreviation: LWD = Leary Webber ditch; SS = Starling Nature Sanctuary; WR: main stem of the White River.

HGM	Site	Sampling period		Carbon dioxide	Methane	Nitrous oxide
				Wet season [a]		
1	LWD-1	04/10 to 05/28	Min - Max	0.23 to 6.04	-0.97 to 0.40	-0.39 to 2.21
			Mean (std)	4.49 (0.22)A[b]	-0.27 (0.11)	0.29 (0.22) B
2	SS	04/15 to 05/26	Min - Max	0.76 to 6.25	-0.96 to 4.42	-0.25 to 2.22
			Mean (std)	3.27 (1.54) B	-0.19 (0.29)	0.17 (0.19) B
3	WR	04/16 to 05/20	Min - Max	1.14 to 3.44	-0.48 to 0.34	0.13 to 6.1
			Mean (std)	2.73 (0.24) B	-0.19 (0.08)	0.62 (0.20) A
				Dry season		
1	LWD-1	8/6 to 9/22	Min - Max	0.37 to 3.95	-0.96 to 0.49	0.34 to 0.54
			Mean (std)	2.8 (0.24) A	-0.31(0.11) A	0.26 (0.13) A
2	SS	9/1 to 9/29	Min - Max	0.23 to 2.53	-0.90 to 0.06	-0.44 to 0.93
			Mean (std)	1.38 (0.58) B	-0.55 (0.21) B	0.14 (0.19) B
3	WR	8/30 to 09/12	Min - Max	0.15 to 5.1	-1.64 to 0.27	-0.15 to 0.46
			Mean (std)	2.63 (0.4)AB	-0.54 (0.24) B	0.20 (0.12) A

[a] Rainfall and temperature: 183 mm and 17 ^oC during the wet season; 24 mm and 24 ^oC during the dry season.

[b] For a given season, mean values in a column followed by different letters indicate significant different ($P< 0.05$) between HGM type.

Table 8.
Summary analysis of variance for the effect of year and hydro-geomorphic (HGM) settings on greenhouse gas fl
buffers. The 2010 data are summarized in Table 7, and the 2011 data are reported in Figs. 2-4. All study sites (3
in 2011) are located in the White River watershed, IN.

	Wet season [a]			Dry season		
	Carbon dioxide	Methane	Nitrous oxide	Carbon dioxide	Methane	N
Analysis of variance, P<F						
HGM	<0.001	0.792	0.003	0.014	<0.001	
Year	0.061	0.022	0.052	0.001	0.002	
HGM x Year	0.316	0.003	0.081	0.308	0.015	

[a] The wet and dry seasons correspond respectively to the months April-May and August-September.